• U C •

FCTUC FACULDADE DE CIÊNCIAS
E TECNOLOGIA
UNIVERSIDADE DE COIMBRA

DEPARTAMENTO DE
ENGENHARIA MECÂNICA

Radial expansion fretting of metallic stems against ceramic femoral head

Submitted in Partial Fulfilment of the Requirements for the Degree of Master in Materials Engineering

Author

Aysu Acar

Advisor

Amilcar Ramalho

Jury

President	**Professor Doutor Bruno Trindade** **Professor at University of Coimbra**
Vowels	**Professora Doutora Ana Paula Piedade** **Professor at University of Coimbra**
Advisor	**Professor Doutor Amilcar Ramalho** **Associate Professor at University of Coimbra**

In the framework of Joint European Master in tribology of Surfaces and Interfaces

tribos joint european master in tribology of surfaces and interfaces
Ljubljana • Leeds • Coimbra • Luleå

Coimbra, July, 2015

Contents

List of Figures

List of Tables

ACKNOWLEDGEMENT

Firstly I would like to thank my supervisor Prof. Amilcar Ramalho for his precious guidance and valuable advices throughout my studies. I am grateful for his constant support even from overseas.

I would also like to thank Miguel Esteves for his help and supervision during characterisation of the test specimens as well as the Reciprocating Fretting experiments and for having patience with all my queries.

I would like to express my gratitude to Erasmus Mundus TRIBOS Consortium for selecting me to be a part of this master program. It has been a memorable experience both academically and personally.

A big thank you to my friends who have been my biggest support during this two years; Catur, Naveed, Tanmaya and especially Geet. It would not have been possible to finish this master's program without your encouragement.

Finally, I would like to thank my family for their continued support in the every step of my life.

ABSTRACT

In this thesis work, radial fretting experiments were conducted in order to characterize the contact mechanism between a metallic stem and a ceramic femoral head. Titanium-6Al-4V, Titanium Grade 2 and Cobalt-chromium flat metal specimens were selected as stem materials against alumina counter-body, replicating a femoral head, with a diameter of 10 mm. The experiments were conducted both with and without saline solution. The latter to simulate body fluid environment effect on fretting mechanism. After experiments, the flat specimens were observed under an optical microscope and SEM. The wear profiles of flat surfaces were characterized by a 3D profilometry. The wear volume without solution results indicated that, cobalt-chromium has the highest amount of wear followed by Ti-6Al-4V and Titanium Grade 2 respectively. When saline solution is in contact, wear volume results were changed significantly. For each stem material, the wear amount increased remarkably as compared to the in dry condition. In addition, Titanium grade 2 has a higher wear volume than Ti-6Al-4V while cobalt-chromium has the highest amount of wear. SEM observation was performed to see oxidation and/or corrosion traces on the contact surfaces. The stick-slip regimes of worn surfaces induced by radial fretting were analysed by SEM images. It can be concluded that in both conditions, titanium alloys showed better wear properties than the cobalt-chromium alloy when used against an alumina ball.

RESUMO

O presente trabalho incidiu sobre a caracterização do mecanismo de contacto entre a haste metálica e a cabeça cerâmica do fémur através de fretting de expansão radial. A geometria do contacto foi do tipo esfera-plano. Foram selecionado três materiais: duas ligas de titânio - grade 5 (6Al-4V) e grade 2 (CP titanium) e uma liga de crómio-cobalto sendo o contra corpo usado uma esfera de alumina com 10 mm. Os ensaios foram realizados com e sem presença de solução salina, sendo esta solução usada para simular o efeito dos fluidos corporais no comportamento ao fretting destes materiais. Após os ensaios, todas as amostras foram observadas em microscopia ótica e Microscopia Electrónica de Varrimento (MEV) tendo as respetivas marcas de desgaste sido caracterizadas por perfilometria 3D. Os resultados sem solução salina indicam uma menor resistência ao desgaste por parte da liga de crómio-cobalto seguida da liga titânio grade 5 e finalmente a liga grade 2. Quando a solução salina é adicionada o volume de desgaste aumenta significativamente em todas as amostras, quando comparados sem solução salina. Ainda, na presença da solução salina, o material que passa a ter maior resistência ao desgaste é a grade 5, mantendo-se o restante comportamento. A observação em MEV permitiu a análise da oxidação/corrosão das amostras em cada ensaio, assim como as zonas de stick-slip. Em suma, conclui-se que o comportamento de desgaste das ligas de titânio é superior à da liga de crómio-cobalto quando testados contra esferas de alumina.

1. INTRODUCTION

Among the many public health issues, prevalent these days, the ageing of population, abnormal development and damage due to injuries or diseases like arthritis are of immense relevance. Due to this reason, the hip replacement surgery has gained vital importance over the time. Orthopaedic surgery, by restoring mobility and providing pain relief, has the potential to enhance the quality of life of people. Prostheses for replacing arthritic knee and hip joints are the main orthopaedic implants which are currently in use in the industry. About half a million people around the world undergo Total Hip Arthroplasties (THA) every year [1].

The anatomy of the natural hip comprises of a femoral stem (thigh bone), a femoral head on top of it which articulates against the acetabular cup in the acetabulum (Figure 1). In case of an arthritic hip joint, the lubricating cartilage between the cup and the head gets damaged making movement very painful for the patient. THA is required when the entire joint gets damaged and the damaged parts need removal or replacement by an artificial prosthesis.

THAs, however, require further progress even though they remain one of the most successful operations in all of medicine. It is believed that, approximately 10% of THAs require a "re-intervention" after 10-15 years [2]. Relative motion may occur in the stem surface, on the stem/bone or cement bone side and on the contact between the stem and the femoral head due to the daily human gait and significant difference of mechanical properties. As a result there is a generation of wear debris from the materials used in the prosthesis which subsequently reacts with the adjacent tissues. This reaction has the potential to have an adverse effect on the longevity of the THAs. Along with fretting wear, corrosion has also been identified as one of the main mechanisms responsible for the release of particles in the form of debris[3].

Fretting can affect the fatigue resistance of the material, inducing wear and cracking. It is a wear process that occurs when there is a small amplitude cyclic motion of two solid surfaces in contact. The femoral stem used for THAs mainly comprise of three different metal alloys, namely cobalt-chromium alloy, titanium alloy or austenitic stainless steel. In order to avoid "re-intervention" and to improve the lifetime duration of implants, it is imperative that to conduct more studies on orthopaedic implants [1].

The work in this thesis focuses on fretting in the contact between the stem and the femoral head. In this kind of tapered contact, the displacement is quite small. Because of this reason radial fretting was chosen over other fretting types as the field of study in this work.

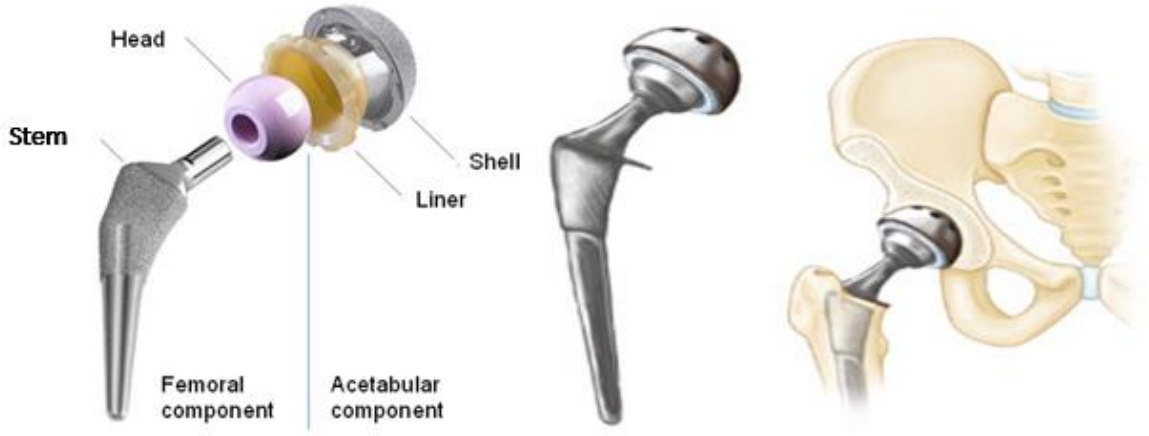

Figure 1 Total hip replacement components (Left) the individual components of a total hip replacement. (Centre) The components merged into an implant. (Right) The implant as it fits into the hip [4]

1.1 Identification of the Public Health Evidence and Research Requirements

Advancement in joint replacement surgeries has certainly been a great medical milestone. Especially total hip replacement surgeries are well established procedures that enhance the quality of life of patients by not only lessening the pain, but also improving their activity levels. Every year about 400,000 hip joint replacement surgeries are done worldwide [1]. According to the National Joint Registry's annual report almost 90,000 replacement procedures were recorded in just England and Wales in 2013 [5].

Total joint replacement lasts approximately 15-20 years and despite the fact that joint replacement surgery has been remarkably successful, almost ten percent of the implants suffer failure and need to be replaced with new components with a second surgical procedure [6]. Annual failure rates provide information about the longevity of implants and according to the current data, for hip and knee replacement, the annual failure rate is between 0.5-1.0 % [2].

There are many reasons that can cause complications in hip replacement; dislocation, loosening of stem, infection, osteolysis, metal sensitivity etc. [7].

Osteolysis is one of the significant problems that limits the expected life of a replacement implant. Bone resorption, due to wear particles and corrosion products, causes loosening of implants and subsequently reversion of prosthesis. It occurs more often around the acetabulum than the femur [7,8].

Metal sensitivity is one of the problems that occurs due to metal release from the implant into the body environment causing immune reactions and affecting approximately 10-15% of the population. It can cause skin hives, eczema, redness and itching of the body [9].

Metal poisoning occurs due to the release of the metal particles into the body resulting in damage to tissues, bone and nervous system or causing implant failure. Especially in case of hip implants, for metal-on-metal contacts, a release of cobalt-chromium ions into the bloodstream which, subsequently causes toxic level increase in the body is observed [10].

When a metal substance is released to the body environment, the results can be damaging. The degradation of orthopaedic implants can be caused by mechanisms of different forms of corrosion including general, galvanic, intercrystalline, crevice, corrosion fatigue, and stress corrosion combined with fatigue and fretting corrosion. Among the other mechanisms, fretting, wear and the maintenance of passive film of a highly corrosion-resistant implant material also leads to the degradation of orthopaedic implants [11].

The main focus of this work is to study the effect of radial fretting on metal stems against ceramic femoral heads.

1.2 Framework

The title of the undertaken project is "Radial expansion fretting of metallic stems against ceramic femoral heads" and this work is divided into 5 chapters. In the first chapter, a brief introduction to this work, followed by a description of the identification of the public health evidence. A detailed literature review referring to the definition of the problem, existing approaches and the establishment of findings from different researchers was presented in the chapter titled, State of the Art. The following chapter explained the selected materials, the purpose of using different characterisation equipments and the experimental techniques employed in this project. Experimental results, comparison graphs and optical and SEM images were used to define, discuss and correlate with existing literature and established protocols in the fourth chapter. Finally, the work was completed with the brief conclusion and some suggestions for possible future studies in the same area.

2. STATE OF THE ART

2.1 History of Total Hip Arthroplasty

In order to achieve a painless, stable and mobile joint implant with a longer lifetime; many combinations of materials and designs have been considered in the past 40 years. Gluck performed the first total hip replacement using ivory in 1890 [12]. The prosthesis, in this case, was held with glue. Early attempts to use a rubber component were rendered unsuccessful by Delbet in1919 [13]. Two decades later in 1939, an interpositional arthroplasty, initially made of glass but later modified to celluloid, Pyrex, Bakelite and Vitallium, was described by Smith-Peterson [14]. A rapid progress in the use of materials and design was made during this time and the first breakthrough came in 1966 when McKee and Farrer described a metal-on-metal hip with stainless steel [15]. This was modified by Charnley in 1967 to include a low-friction high molecular weight polyethylene cup [16]. Gradually by 1968, the superiority of the cobalt-chromium alloys over steel components was established. Around this time, the concept of low friction arthroplasty using both cemented femoral and acetabular components, with a plastic bearing surface and polymethyl-methacrylate (PMMA) for fixation was introduced by Charnley. This prosthesis remains the gold standard in hip replacement even today. Ring, in 1968, developed cementless cup components with long pelvic anchoring screws after pointing out the disadvantages of using PMMA cements [17,18]. Dipisa, Sih and Berman suggested that thermal necrosis of bone in contact with PMMA may be partly responsible for the loosening of the total hip arthroplasty [19]. Further studies have also revealed that movement at the interface of bone and cement cause PMMA debris and accelerates wear of other components in metal-plastic systems. In order to achieve higher wear resistance properties, scientists have started using ceramic implants such as alumina and zirconia ball [18].

2.2 Implant Materials

In orthopaedic surgery, firstly stainless steel was introduced to the medical industry from about 1926. Since then they have been one of the major implant alloys used in this industry. Recently, however, with the development of new manufacturing techniques, cobalt-chromium and titanium alloys joined the orthopaedic implant industry with better specifications [1].

Cobalt-chromium alloys, in their early assessment as orthopaedic implants, presented an admirable wear and corrosion resistance with excellent biocompatibility but poor machinability. Finally, advancement in machining techniques and special tools paved the way for the development and the production of these alloys as one of the more successful orthopaedic implant materials [20–22].

Commercially pure titanium and titanium alloys are newer than their stainless steel and cobalt-chromium counterparts in the orthopaedic implant history. The research for these alloys in the medical industry was first launched around 1970s after these alloys were already established as an important material for the aerospace industry. Low density, high strength with good ductility, low modulus and biocompatibility properties made the titanium alloys an excellent choice as an orthopaedic implant material [23,24].

2.3 Fretting and fretting modes

The ASM Handbook on Fatigue and Fracture [25], describes fretting as "a special wear process that occurs at the contact area between two materials under load and subject to slight relative movement by vibration or some other force."

A lot of parameters need to be considered whilst modelling fretting behaviour. Firstly, and most importantly, the contact geometry, such as pin on plane or ball on flat (Hertz) and so on, needs to be examined. Secondly, consideration must be made for the loading conditions including pressure and the type of load. Thirdly, the kinematics of the contact zone need to be studied. This involves the study of the relative displacement magnitude, slip direction, maps of slip, and rate of deformation and so on. Fourthly, the study of the effect of temperature on the materials and the interfacial friction is required. Finally, the parameters of roughness of the bodies in contact, frequency and the number of cycles is considered [5].

Depending on the relative movement direction, there are four fretting modes: tangential fretting (a), radial fretting (b), rotational fretting (c), and torsional fretting (d). They are shown in the figure 2 respectively [26].

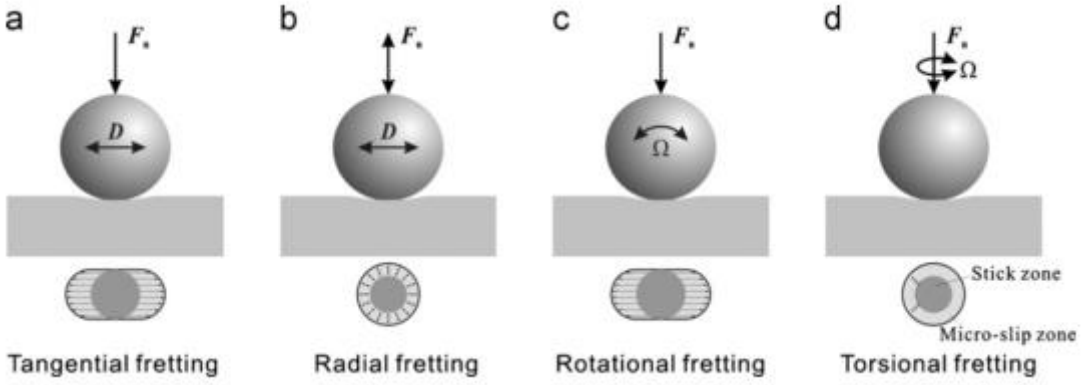

Figure - 2 Four simple fretting modes under the contact of ball-on-flat [26]

In the literature, tangential fretting mode is the most studied compared to the other modes while not a lot of research work exists for the radial fretting mode. For similar fretting situations Mindlin et al. [27], have emphasised the aspects concerning contact mechanics and some experiments were conducted by Johnson [28] in the early 1960s [29].

2.4 Fretting Maps

The essential kinetic information is given by the F_t - D (tangential force vs. displacement amplitude) curves for tangential fretting tests while for radial fretting test this curve is called F-D (alterative normal load vs. indentation displacement) [26].

Figure 3-a) indicates a linear F_t - D curve which means the centre of the contacts sticks while micro-slip arises at the edge of the contact as explained by Mindlin et al [30]. This curve is correlated with a partial slip running status and coordinated by elastic deformation. With the initiation of elasto-plastic deformation between contacts, F_t - D curve forms an elliptical shape even though running status is still partial slip (Figure 3-b)). Finally, the gross slip fretting running status is indicated by a parallelogram shaped F_t - D curve as can be seen in figure 3-c) [26].

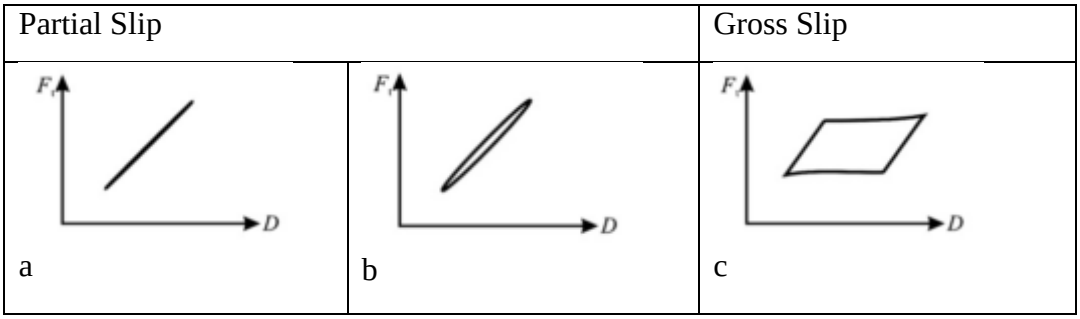

Figure - 3 Fretting running status for tangential fretting [26].

The fretting map concept was first studied by Vingsbo and Söderberg [31] and they proposed three different regimes; stick regime, mixed-slip regime and gross slip regime respectively corresponding to linear, elliptic and parallelogram F_t -D curves.

However, progression of the F_t - D curves during actual fretting is uncertain with complexity. So, Zhou and Vincent [26,32], came up with three new regimes, namely, partial slip regime, slip regime and mixed regime which correlated to lower displacement, higher displacement and medium displacement amplitudes respectively. F_t - D curves in the partial slip regime corresponds to linear and elliptical shape while those in the slip regime have a parallelogram shape. In the mixed regime, running status alters between gross slip to partial slip and eventually gross slip [33].

The difference of deformation behaviour and contact stress-strain distribution in varied contact zones is actuated by the difference of fretting running modes. Subsequently, the different fretting kinetic behaviours, damage morphologies and mechanisms are induced by the said different deformation processes and stress-strain relations [26].

2.5 Radial Fretting

Radial fretting is generated by varying the normal load or thermal cycling while the surfaces stay in contact and impact effect doesn't occur [34]. In order to refrain from impact effect, the minimum value of cyclic applied loads must be positive [34–36], which generates a sticking zone in the centre. Due to sticking area is at the contact centre, only at the edge of the area, micro-slip is seen in shape of annularity. Obviously, radial fretting always runs in partial slip regime. Figure 4 shows the stick zone, micro-slip zone and wear zone of contacts.

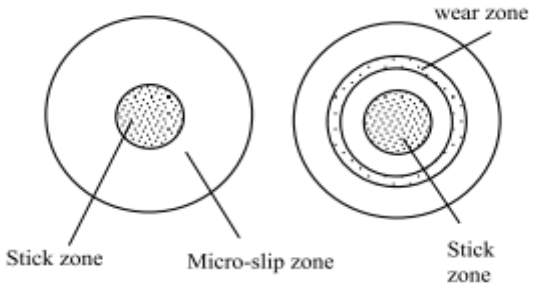

Figure - 4 Radial fretting contact area zones [36]

As mentioned before, the important kinetic information is obtained from the F-D (alterative normal load vs. indentation depth) curves for radial fretting. As can be seen from Figure 5, F-D curves have two different shapes; linear and elliptical which correspond to elastic and elasto-plastic deformation between contacts respectively [34–36]. Depending on different materials and different deformation behaviour, curve shapes can be altered between linear and elliptic cycles.

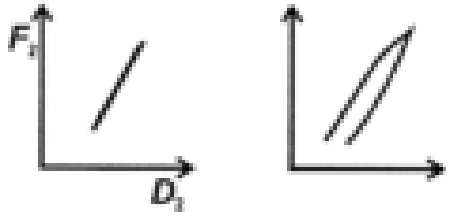

Figure - 5 Force vs. Displacement curves for radial fretting; closed and elliptic cycles[26].

In radial fretting, due to the oscillatory normal load applied to a Hertzian contact, a cyclic loading and unloading occurs in the contact area [37].

In theory, in order to get a stick zone in the contact, d_{min} should be obtained and the only area where the micro-slip occurs is between d_{max} and d_{min} [34]. Upon consideration of the Hertzian contact, the normal load alters between P_{max} and P_{min} values during a cyclic motion. These values define the contact area radius d_{min} and d_{max} corresponding to P_{min} and P_{max}. However, it is better to emphasize that fretting is caused by normal load variation and causing the micro-slip to possibly occur when two dissimilar materials are in contact[38]. This can be seen in the stages of the contact zones during a loading cycle in Figure 6.

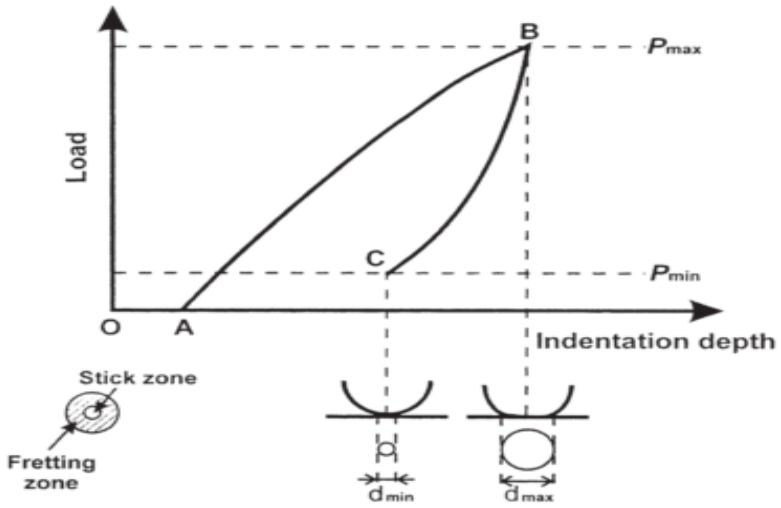

Figure - 6 Variation of normal load and contact area for the first cycle [34]

Investigations of radial fretting in literature appears to be quite rare. Recently, further research has been done in China, involving radial fretting tests on coatings, steel and ceramic components although these studies have not been enough to establish a model to explain radial fretting phenomena [29].

Currently, there are not many theories or models existing in order to support radial fretting. However, the Hertz Theory, Mindlin theory and the Hamilton model play an important role in understanding and explaining the characteristic of fretting behaviour.

Even though Hertz theory is helpful for the study of the fretting phenomena, its limitations, such as restrictions on the type of contact and its implementation only in cases where the friction is zero, prevents its applicability for the study of radial fretting.

For subjective approaches, analysis of Mindlin and Hamilton provide an understanding of radial fretting; however, for an objective perspective, these models are not applicable to explain radial fretting phenomena [39].

Therefore, for interpreting such kinds of fretting behaviour, there is a necessity of numerical models, including finite element analysis, with a combination of experimental modelling.

2.6 Damage Mechanism

The generation of particle debris is a major concern in arthroplasty. The long-term durability of contemporary total hip replacement arthroplasty is limited by the biological response of the tissues to the wear debris. Studies have shown billions of particles per gram of tissue are contained in tissues in the proximity of a failed joint prosthesis. These particles are mostly classified as metallic, polymeric or ceramic with most results being reported on metal debris from CoCr and titanium [40].

The damage to a solid surface leading to progressive loss of material due to the relative motion between that surface and a contacting body is defined as wear. Neither creep and plastic deformation nor corrosion can be directly related to wear. The former does not produce any wear debris and the latter can take place without any mechanical activation [41]. Wear is described mainly by the relative motion responsible for producing it and by the physical mechanisms responsible for removing or displacing the material in wear. Adhesive wear occurs when the bonds that form between two surfaces are broken leading to formation of fragments that get transferred from body to counter-body resulting in flaking and pitting and causing surface damage [42]. Abrasive wear is a result of the removal of material from a surface by hard asperities on the counter-body or the third body that is trapped between two surfaces in contact [42]. Corrosive wear is mainly caused by a combination of mechanical wear and chemical reaction [42]. Occurrence of repeated sliding or rolling over the same wear track results in fatigue wear [40].

Fatigue strength of a material is decreased by fretting performed under cycling stress. This can result in fretting fatigue. In the fretting zone, fatigue crack initiation can be seen and consequently, so can crack propagation into the material. In the cyclic loading zones, it is not essential for the implant to be loaded in the plastic deformation range for fatigue crack development. Also fatigue crack initiation can be seen in the surface of the implant when local stress occurs under cyclic loading in the elastic deformation range. The progress of the fatigue damage is developed by the number of the load cycles and strength of the loading [11].
.

Fretting wear and fretting fatigue are two of the consequences of the fretting mechanism [32]. Fatigue causes plastic deformation and separation of particle from the surface, depending on the behaviour of materials in contact. For mixed regime, main damage mechanism is cracking (fretting induced fatigue), and for slip regime is material loss (fretting induced wear) [26]. These failure mechanisms can be seen in radial fretting. As the contact centre always remains in contact, wear and fatigue are seen in the outer ring of the contact [35]. According to the radial fretting experiment results obtained by Zhu et al., relative motion and wear produced were much less for radial fretting compared to data from literature [34].

3. MATERIALS AND METHODOLOGY

3.1 MATERIALS

Materials used as hip joints should show response in terms of various properties in order to last a long-life duration without any surgical operation in patients.

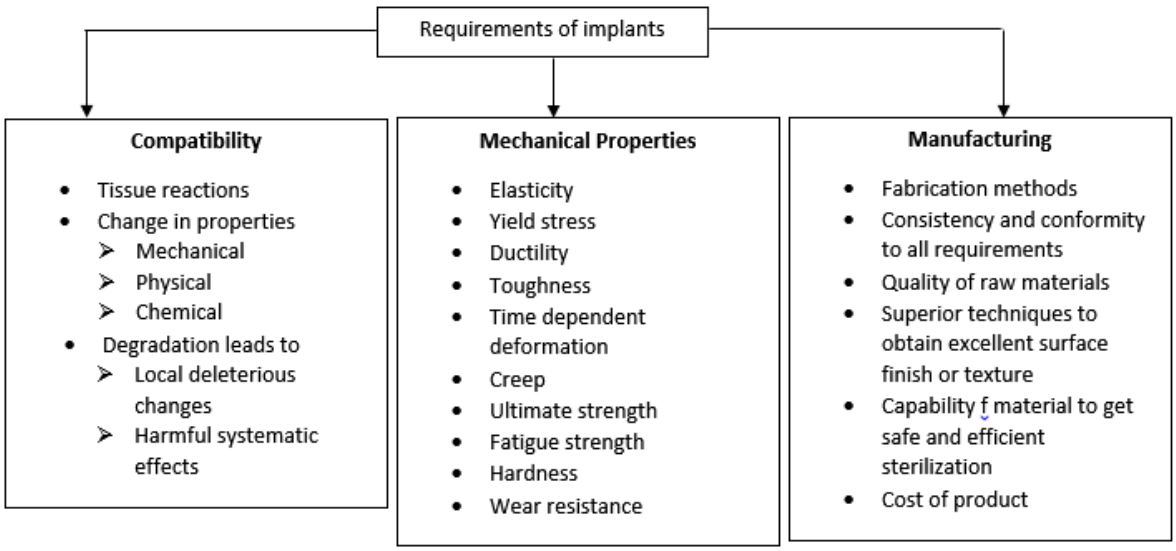

Figure 7-Requirements of implants [43].

First of all these properties is biocompatibility. A biocompatible material should not cause any adverse chemical reaction and should remain chemically stable at body temperature and environment. Also, it can be described as "the quality of not having toxic or injurious effects on biological systems"[44,45].

In addition, biocompatibility includes corrosion resistance, which has an important role in the degradation of implants due to the metal ion release particularly in total hip replacements [44].

Also, hip replacement materials should have excellent fatigue resistance and satisfactory strength to stand cyclic loading because, according to researches, the average non-active person's hip is subjected to approximately 1 to 2.5x 10^6 cycles of stress in a year.

One of the other major properties of a hip replacement material is wear resistance. Wear debris generation not only causes toxicity in body but also promotes to degredation of orthopaedic implants [46].

A low elastic modulus is an important factor to minimize bone resorption. The bone has a Young's modulus of 17 GPa (2.5×10^6 psi). The modulus difference between an implant material and the bone can cause unequal distribution of the load. If the modulus of the material is lower than the bone, the remaining part of the bone which surrounds the implant, experiences a higher load. If the implant stiffness is significantly higher than the bone, then the bone is exposed to a lower load than it experienced before. This phenomena is known as stress shielding [47,48].

The various implant materials used in orthopaedic surgery are presented according to their mechanical and physical properties in the following table.

Table 1 Composition of implant metals and alloys used in orthopaedic application [1,49]

Material	**Composition wt. %**									
	Al	C	Co	Cr	Fe	Mn	Mo	Ti	V	O
Cobalt-chromium-molybdenum	…	0.2	balance	27-30	1	1	5-7	…..	…	…
Titanium Grade 2	…	0.1 max	…	…	0.3 max	…	…	balance	…	0.25 max
Ti-6Al-4V	5.5	0.08	…	…	0.3	…	…	balance	3.5-	…

Table 2-Physical and mechanical properties of implant metals and alloys used in orthopaedic application[1]

Materials	**Physical and mechanical properties**			
	Density(g/cm3)	Young's Modulus(GPa)	Tensile Strength (MPa)	Fatigue Stress, (MPa)
Cobalt-Chromium-Molybdenum alloy	7.80	200	665	290
Titanium Grade 2	4.51	105	344	300
Ti-6Al-4V	4.40	111	900	380

For the radial fretting experiment there were three different biomaterials used as a metallic stem of the hip replacement; Titanium Grade 5 (Ti-6Al-4V), Titanium Grade 2 (commercially pure) and Cobalt-chromium-molybdenum alloy.

3.1.1 Titanium Alloys

Titanium alloys have great biocompatibility and mechanical properties in order to be used as femoral stems in hip replacement surgeries, especially, due to the stable oxide layer (TiO_2) formed on its surface, which makes its corrosion resistance superior to the other metals and alloys used in biomedical applications. In addition, its low elastic modulus reduces the shielding effect on the bone. All these properties makes titanium alloys attractive in their use as an implant material. [45]

Table 3 Designations and nominal compositions of titanium alloys

Common alloy designation	**Nominal Composition,%**	**ASTM Grade**	**Alloy Type**
Grade 2	Unalloyed Titanium	2	α
Ti-6-4	Ti-6Al-4V	5	α-β

3.1.1.1 Ti-6Al-4V (Grade 5)

It is the most common Ti alloy used in biomedical devices. It has a chemical composition of 6% aluminium, 4% vanadium, 0.3% iron, 0.2% (maximum) oxygen, and the remainder titanium.

Ti6Al4V enables the formation of a passive oxide layer on its surface and due to this oxide layer it is one of the primary choices for a femoral stem material. Among its corrosion resistance advantages, it has a superior wear resistance which can be improved by surface treatment such as nitriding and oxidizing. [50,51]

The alloy Ti-6Al-4V has a higher toughness and improved fatigue resistance with easier weldability and machinability than CP titanium [48,52].

3.1.1.2 Titanium Grade 2 (Commercially Pure Titanium)

CP Titanium Grade 2 (98.9 to 99.6 % Ti) has excellent formability and corrosion resistance with moderate strength. It has a strong stable oxide layer formed on the surface which is exposed to oxygen instantly. Even if this oxide layer is damaged, it re-generates itself in the presence of air or a moisture environment. In addition, CP Ti Grade 2 has resistance to stress-corrosion cracking in aqueous solutions [49].

Presence of interstitial elements like O, N, and H affect the mechanical properties of CP Ti alloys. Higher O content gives a higher solid solution strengthening while lower O content means low strength but higher ductility. Depending on the variation of the impurity level CP Titanium grades can vary. Grade 2 takes place between Grade 1 and Grade 3 in terms of strength due to its relatively low levels of interstitial elements [45].

3.1.2 Cobalt-Chromium-Molybdenum Alloys

Cobalt-based alloys have a good balance between mechanical properties and biocompatibility which helps them to find usage in the biomedical industry. Strengthening of the cobalt-chromium alloys is attained by the addition of refractory materials, such as molybdenum and

tungsten, as well as by the addition of carbon. The addition of the refractory metals cause solution hardening whereas, that of carbon leads to dispersion hardening and grain boundary stabilization. Both these processes ultimately result in improved mechanical properties of the aforementioned alloys [53]. As a result of the addition of carbon to these alloys, a carbide phase mainly in the form of $Cr_{23}C_6$, is formed. [54]

One of the well-known cobalt-based alloys is Cobalt-Chromium-Molybdenum alloys. They have good wear resistance, high strength and good corrosion resistance particularly in chloride environments which bears a relation to its bulk composition mainly presence of high chromium and surface oxide [45].

3.1.3 Alumina

Ceramic materials such as alumina and zirconia have significant use in the biomedical implant industry as a femoral head. With a very smooth surface achieved by polishing, the wear properties of ceramics can be improved. However, during manufacturing, the microstructure of the femoral head must be controlled cautiously in order to get a uniform and small grain size. In addition to avoid removal of particles from the ceramic material, the femoral head and cup should fit properly into one another [55].

For radial fretting experiment alumina ball with a diameter of 10 mm was used against titanium grade 2, Ti-6Al-4V and cobalt chromium flat specimens.

3.1.4 Saline Solution

A balanced salt solution with 0.9 % weight of sodium chloride concentration was used to replicate the body fluid in order to assess the performance of the materials.

3.2 EXPERIMENTAL PROCEDURE

3.2.1 Sample Preparation

In order to see the radial fretting mark on both the optical microscope and the Scanning Electron Microscope (SEM), sample surfaces should be prepared thoroughly. Preparation was initiated with grinding of samples, resulting in their abrasion, using sandpaper grid 320, 600, 1000 and 2500 respectively. It was followed by polishing the samples with a diamond paste and subsequently, titanium grade 2 and Ti-6Al-4V's surfaces were finished with colloidal silica paste on a nap cloth. Before starting the experiment each specimen was cleaned with ethyl alcohol.

3.2.2 Mechanical Characterization

3.2.2.1 Hardness Measurement

Micro indentation hardness test was performed on all three flat samples by Struers Duramin instrument. Vickers indenter was used under 1 kgf load during 15 seconds in a single mode of the instrument. The test was performed 10 times on each specimen and an average value was taken in the end.

3.2.2.2 Roughness Measurement

In order to obtain surface roughness MUTITUYO SURFTEST SJ-500 surface measuring instrument is used. Each sample was measured 5 times and their average value were calculated in the end. There are 4 parameters used for measurement; R_a, Rq, Rz and $R_{sk.}$

R_a is the arithmetic average height (μm) that most used parameter, provide general information of height variations. R_q is root mean square roughness which has importance characterize the surface roughness by statistical method. R_z, according to ISO system definition it gives the difference between average of five highest peak and the five deepest valley within a sampling length. Rsk is a measure of the asymmetry of the amplitude density curve. Profiles that has removed peaks or deep scratches give negative skewness while, high peaks and filled valley have positive skewness [56].

3.2.2.3 Etching

The etching process is used for the metallographic analysis of a material. After etching, the material microstructure can be seen clearly under optical microscope. However, before etching the material plane surface area should be polished properly, free from any dirt and surface deformations like scratches [57]. Table 4 indicates three different etchants were prepared for three different samples.

Table 4- Etchants [58,59]

Metal/Alloy	**Etchant**	**Instructions**
Ti-6Al-4V	10 ml HF, 5 ml HNO_3,85 ml H_2O	Etch 15 seconds
Titanium Grade 2	1-3ml HF, 10 ml HNO_3, 30 ml lactic acid	Etch 5- 20 seconds
Cobalt-chromium alloy	100 ml HCL , 20 ml 3% H_2O_2	Etch immediately after polishing, immerse, and swab 2-4 min

3.3.3 Radial Fretting Experiment

As mentioned in the previous section, radial fretting is caused by a small amplitude oscillatory motion and its basic principle is periodic application of a normal force to a ball-flat contact. The test rig was designed and built in the department of Mechanical Engineering by Prof. Amilcar Ramalho. It was developed to produce radial fretting for ball-on-flat configuration. An illustration of the test apparatus is shown in figure 8 and figure 9.

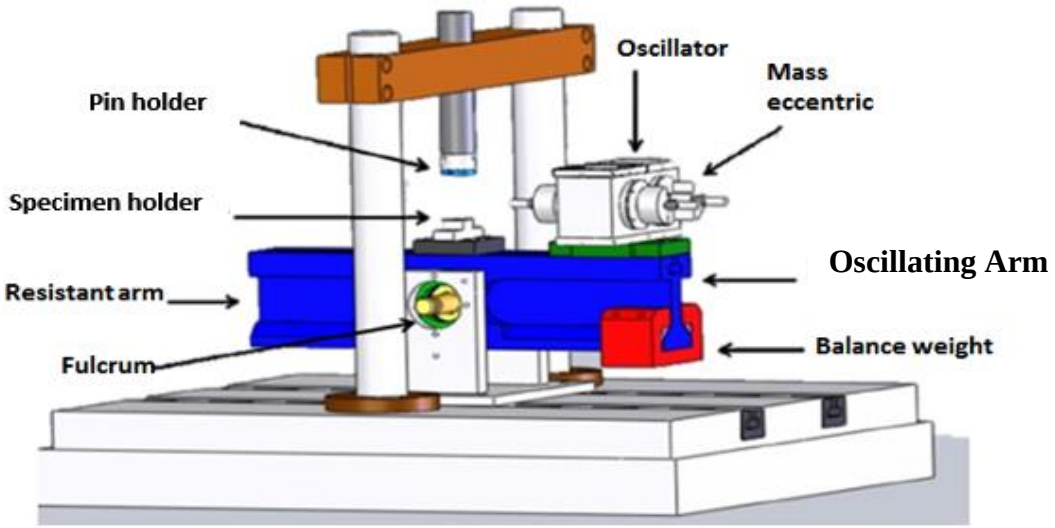

Figure 8-Three-dimensional view of the radial fretting machine [39]

The radial fretting test equipment consists of four synchronized eccentric masses which are positioned on the oscillating arm, producing vibrating motion. The high inertia of these masses generates force variations to the oscillating arm. The mass eccentric replicates the circular motion generated by the electric motor. The test machine is based on a simple principle of momentum, using a lever balance to amplify the force. In order to adjust the amount of applied force, the oscillating arm (distance between the oscillator and fulcrum, *a* (figure 9)) and the resistant arm (distance between ball holder and the fulcrum, *b* (figure 9)) are arranged accordingly.

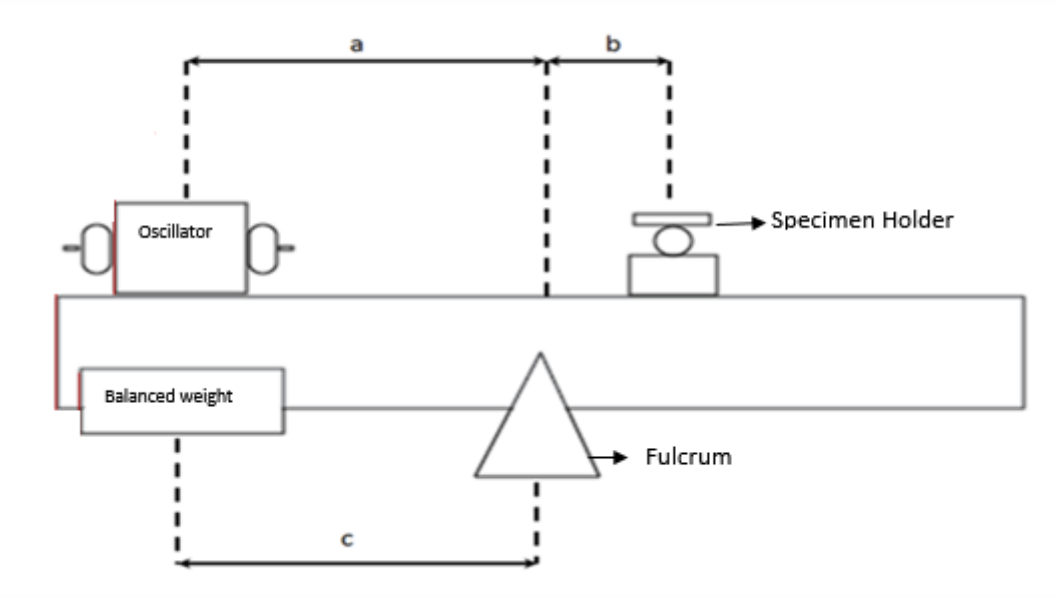

Figure 9-Two dimension figure of Radial fretting machine a; distance between the oscillator and fulcrum, b; distance between ball holder and the fulcrum, c; distance between balanced weight and fulcrum

The total number of laps that the electric motor performs during the test determines the final number of test cycles. The balance weight used, aids in obtaining a preferred static force and its position is adjustable related to the contact. The radial fretting machine system is positioned on a marble plate in order to avoid external vibrations during the test.

The flat specimen was fixed to lower holder while 10 mm alumina ball was fixed to upper holder which was linked to a probe, connected to and synchronized with LabVIEW®. This probe that contains piezoelectric crystals, monitors the entire test thus, making possible to acquire the amplitude of the applied force during contact. During the entire duration of the test frequency, number of cycles and the applied load is monitored and recorded by the software: LabView®. The balance of the moments of the various components gives the average force value.

Prior to reaching the final parameters for the radial fretting tests, a set of preliminary tests were conducted. In these tests, primarily different frequencies, load and number of cycles were used until a fretting mark was observed. However, plastic deformation was resulted every time rather formation of slip rings. Subsequently, it was decided to decrease the load using which the other specifications of the test rig were altered. Therefore, using these tests, the final test parameters for the radial fretting experiment was decided upon (Table 5). The test results for the preliminary tests are attached in appendix.

Table 5-Test parameters for radial fretting experiment

Frequency(Hz)	Contact Force peak to peak (N)	Mass (kg)	Cycle
23	15	2.8	$2x10^6$

3.3.4 Reciprocating Fretting Test

In order to measure the friction coefficient of materials and their energy dissipation, to understand the fretting mechanism, and to apply higher strokes with elastic stresses, a reciprocating test was performed on all three materials. A home-made tribometer was used to obtain data.

The tribometer, used for reciprocating fretting wear test, has a chamber to control the atmosphere of the experiment. It is connected with a pump, humidifier/ desiccator circuits and humidistat/thermometer in order to adjust the relative humidity inside the chamber. Figure 10 is an illustration of the reciprocating test equipment.

Before running the test, the specimen was cleaned in an ultrasonic bath and mounted to the lower holder of Tribometer. A 10 mm alumina ball was then placed into the upper holder and the normal load was applied after closing the chamber. The same test conditions with the oscillating frequency 10 Hz, the number of cycles of 10000, normal load 10 N, humidity 50% and 40 μm imposed displacement; were used for all three specimens.

The normal force, which was applied to the upper holder, was measured by a load cell and a piezoelectric tangential load cell which interrelated the sample to a piezoelectric actuator was connected with the lower holder. The piezoelectric actuator is responsible for stimulation of the tangential movement. Data processing was achieved using LabView® in order to assess the friction force. Reciprocating fretting mark on contact surfaces were analysed on the 3D profilometer and wear volume was calculated with using Gwyddion software and results were studied to rank materials according to their wear properties for hip replacement applications.

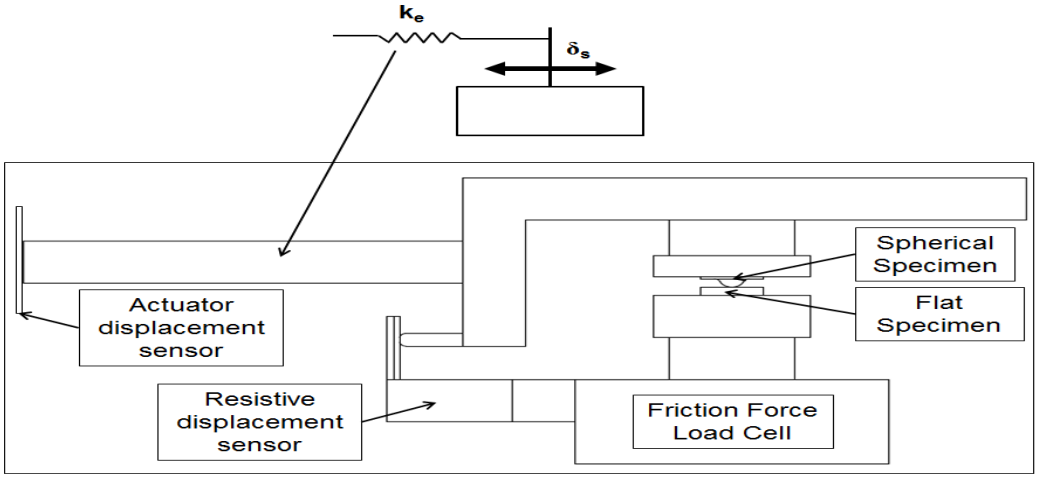

Figure 10-An illustration of reciprocating fretting tester [60]

3.3 CHARACTERIZATION PROCEDURE

3.3.1 Optical Microscope

After the fretting experiment, the samples were cleaned in order to be analysed under the optical microscope. Carl Zeiss®-Epiplan instrument with different magnifications was used to see radial fretting mark on sample surface.

3.3.2 Profilometer

In order to study the three dimensional surface profile and to obtain information on roughness and topography, Mahr® Rodenstock RM600-S profilometer was used. GWYDDION was used to process the data so that the wear volume calculation of the fretting zone could be achieved which, in turn, aids in interpretation of the test results.

3.3.3 Scanning Electron Microscope (SEM)

In order to analyse the surface in detail as well as to observe any surface damage or crack initiation; a Philips XL 30 model SEM was used. In addition, SEM is perfect to detect any trace of oxidation which helps in the interpretation of corrosion, in case of any, on the surface as the specimen is exposed to not only saline solution but also air.

4. **RESULTS & DISCUSSION**

4.1 Micro hardness

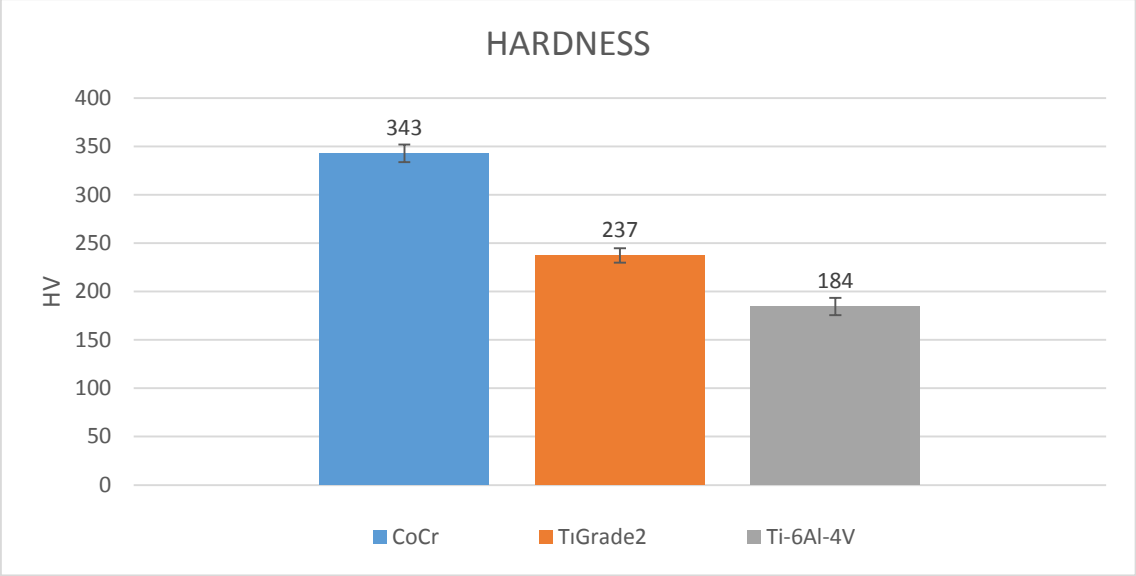

Figure 11 Microhardness comparison of CoCr, Ti grade 2, Ti-6Al-4V

As hardness is considered to be an important property while performing the wear test, so before the radial fretting test, hardness testing of the all specimens is carried out, to correlate also the effect of hardness on the radial fretting after testing. Hardness testing is performed for CoCr, Ti2 and Ti5. Ten hardness values are measured for each specimen, resulting average hardness value of each material is plotted in the Figure 11. Figure 11 shows that CoCr has the highest hardness value of 343 HV while the Ti2 has the hardness value of 237 HV and Ti5 has the hardness of 185 HV. Hardness values of CoCr and Ti2 are similar as found in literature while Ti5 hardness value is much lower from the literature value[1].

4.2 Etching

As explained in methodology section, after etching process was completed specimens became ready for analyses under optical microscope. Figure 12 shows the optical microscope images of three samples after etching. Analysis of the cobalt-chromium-molybdenum alloy microstructure Figure 12(a), suggests that the orientation of the grains are, possibly, a result of the casting process. The microstructure should be dendritic, however unfortunately the etching was not effective to reveal the microstructural features. Figure 12(b) indicates an equiaxed alpha microstructure of commercially pure titanium grade 2. Figure 12(c) exhibits the alpha (white) & beta (dark) microstructures of Ti-6Al-4V.

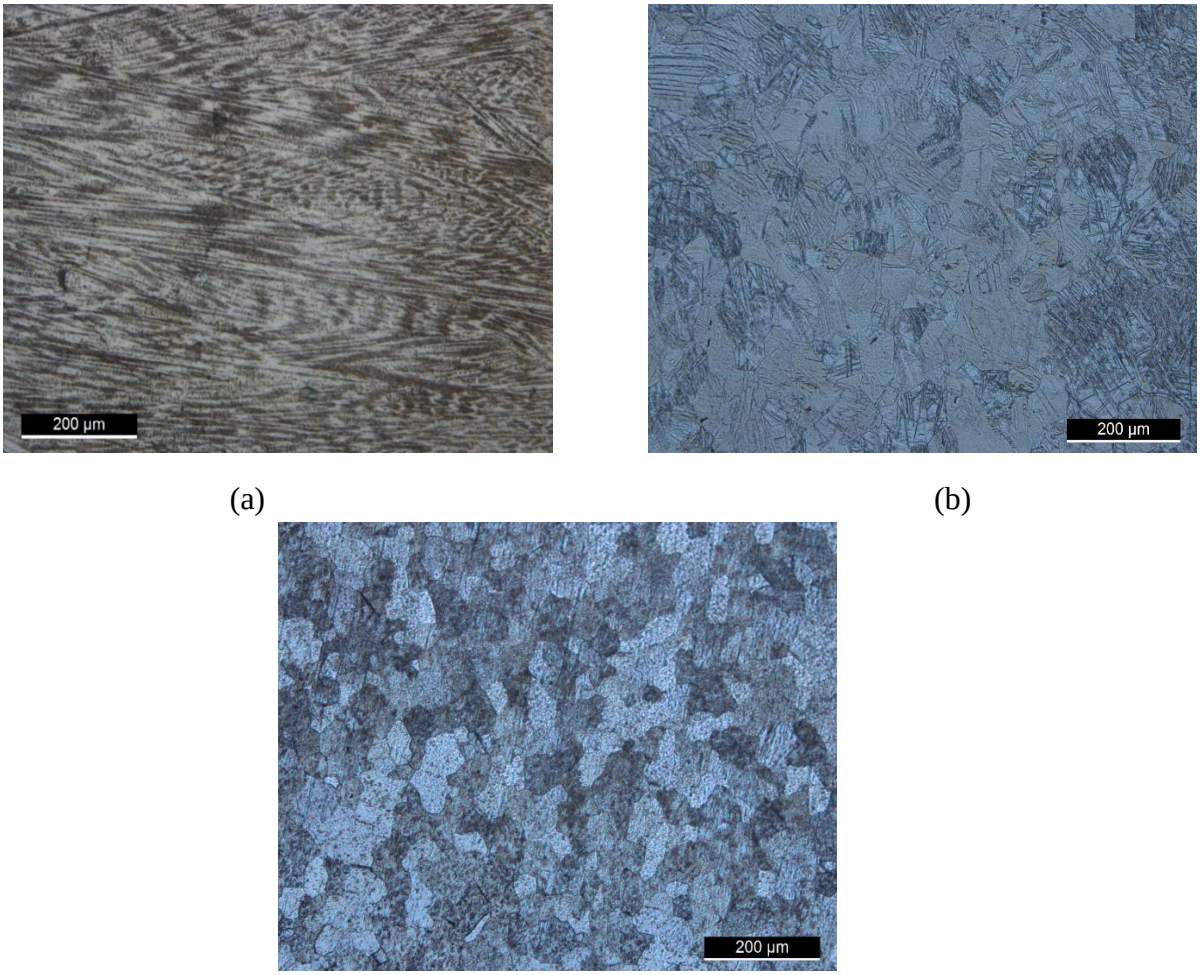

(a) (b)

(c)

Figure 12 Microstructure of (a) Cobalt-chromium-molybdenum alloy, (b) Titanium grade2, (c) Ti-6Al-4V

4.3 Roughness measurement

Roughness measurement for three material are shown in the Table 6. In comparative perspective, titanium grade is slightly rougher than the other materials but according to the literature the surface roughness of Ti having Ra value under 1 µm, is accepted as smooth surface [61]. Due to roughness increase adhesion, generally rougher surface subjected to wear quickly and have higher friction coefficient. Ra values of all materials are close to each other although a bit higher surface roughness will result in the initial higher running in wear.

Table 6 Roughness measurement of materials

	CoCr	Ti 2	Ti-6Al-4V
Ra(µm)	0.127	0.156	0.112
Rq (µm)	0.159	0.190	0.147
Sk	0.055	0.007	-1.250
Rz (µm)	1.063	1.188	0.814

4.4 Radial Fretting Experiment Results

As mentioned earlier, radial fretting is one of the fretting mechanism under small amplitude cyclic motion, where two surfaces are always in contact during experiment, without impact effect. In order to simulate body environment and observe the effect on material, experiments were performed both in Salt Solution (SS) and in the air. Results were analysed to compare three stem material performance under radial fretting condition as well as their performance in the body environment.

Figure 13 indicates a comparison of wear volume of three material under radial fretting in dry condition. Results shows that CoCr has the highest wear volume, while Ti6Al4V has the 2nd larger wear volume and Ti2 shows the lowest wear volume. Wear results cannot be related with the hardness of the materials as apart from the highest hardness of CoCr, it has the highest wear volume. This trend can be supported by the 2-D profiles of worn surfaces shown in Figure 14.

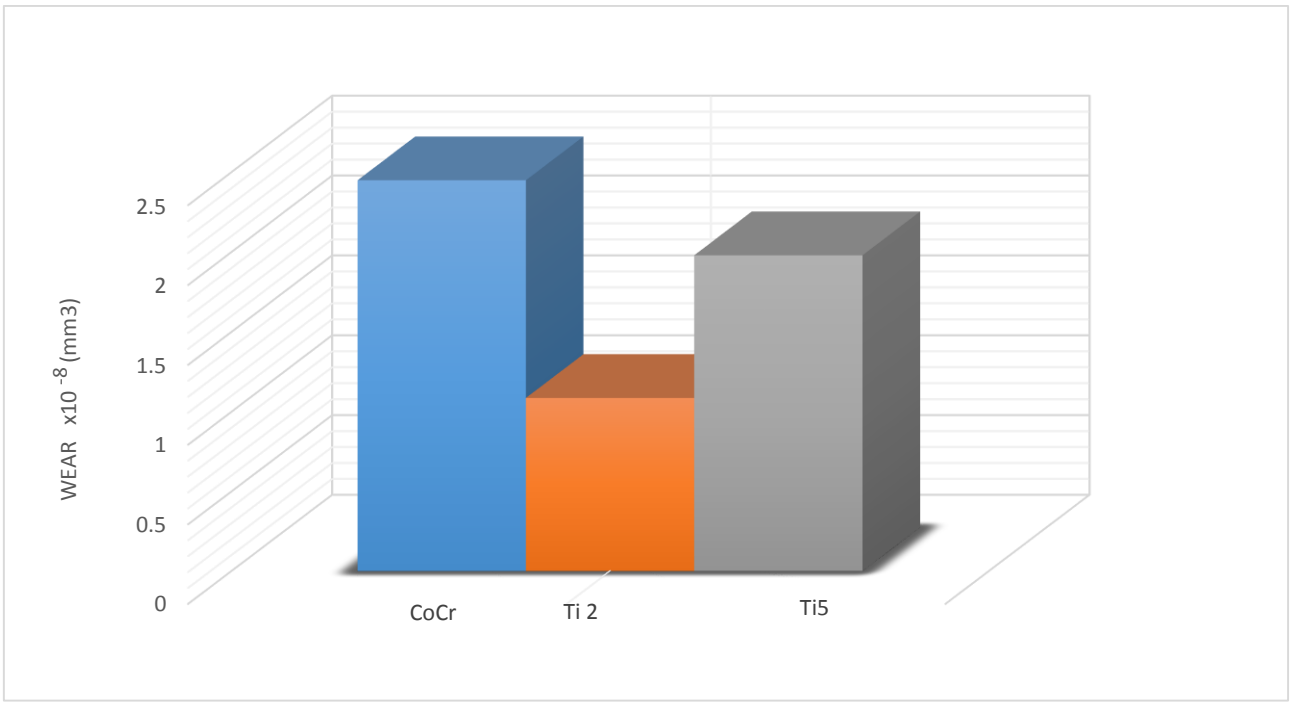

Figure 13-Comparison of radial fretting wear amount-without solution

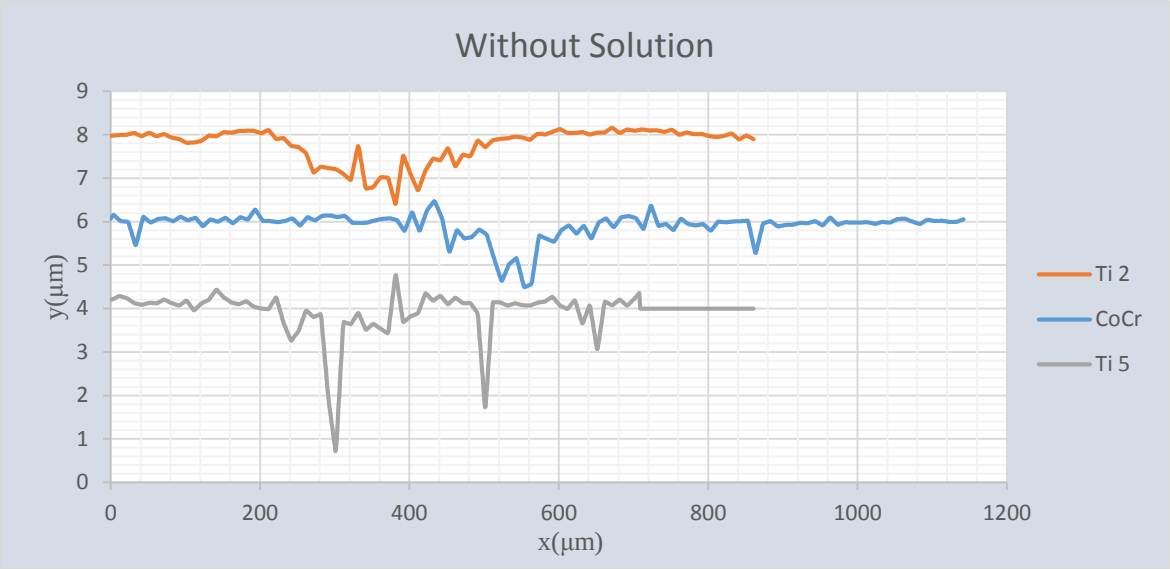

Figure 14- 2D radial fretting wear profiles of materials - without saline solution

Same comparison graphs were made to analyse SS effect on radial fretting wear mechanism and it is seen that results are significantly changed with the environment of saline solution as shown in Figure 15.

Similar to the dry environment results, cobalt chromium has also shown the highest wear amount in saline solution. In this corrosive environment, titanium alloys show better resistance probably due to their protective layer formed by titanium oxide [45]. Remarkably, titanium dioxide showed its effect under fretting motion in saline environment in this experiment.

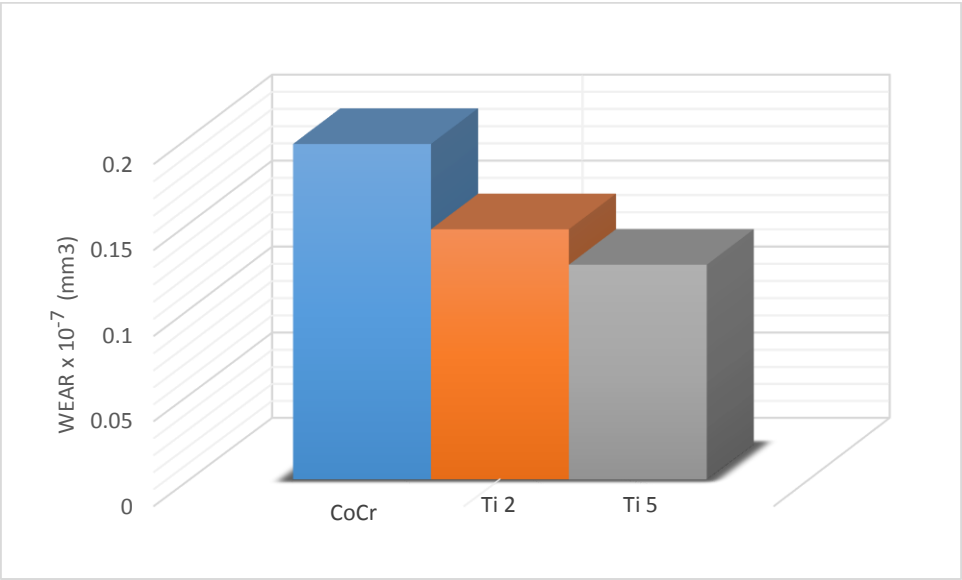

Figure 15 Comparison of radial fretting wear amount-with saline solution environment

In Figure 16 shows that wear depth is clearly much higher in saline solution than that in dry condition.

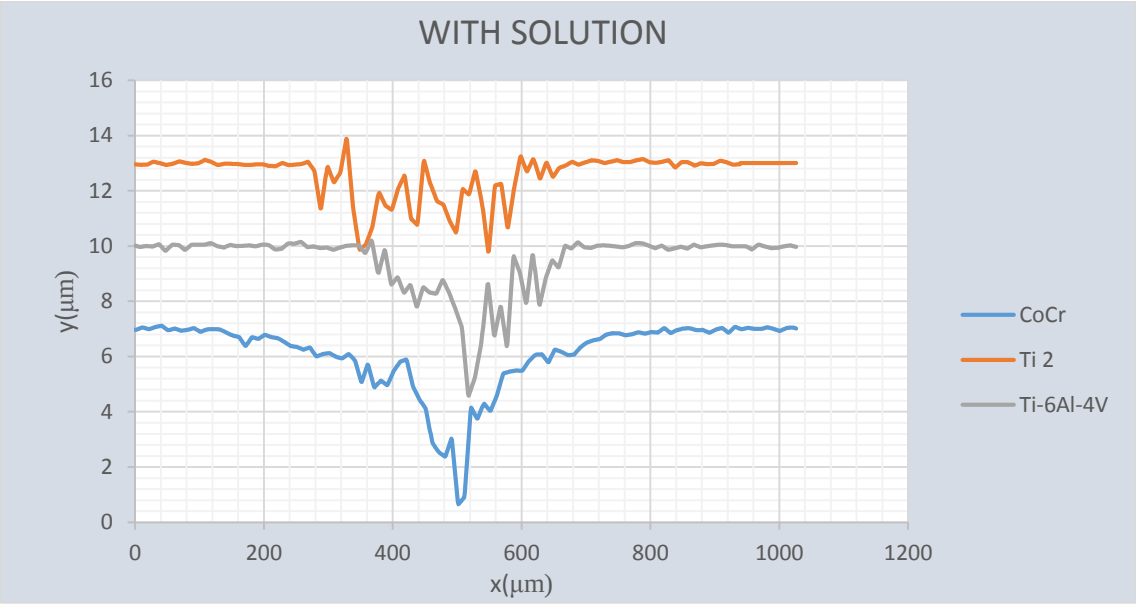

Figure 16 -2D Radial fretting wear profile of stem materials in saline solution

4.5 Comparison of Wear Volumes of CoCr, Ti2 and Ti-6Al-4V in SS and air environment

Figure 17 indicates a comparison of the two different environment‘s effect on radial fretting wear amount. There is a remarkable difference of wear amount in the two environments.

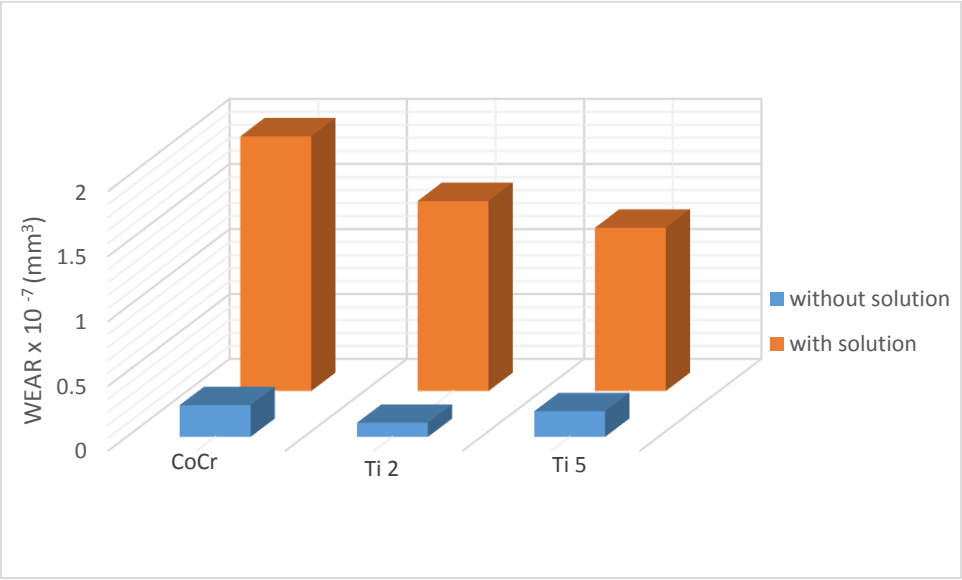

Figure 17 - Wear volume comparison of with SS and without SS for all three materials

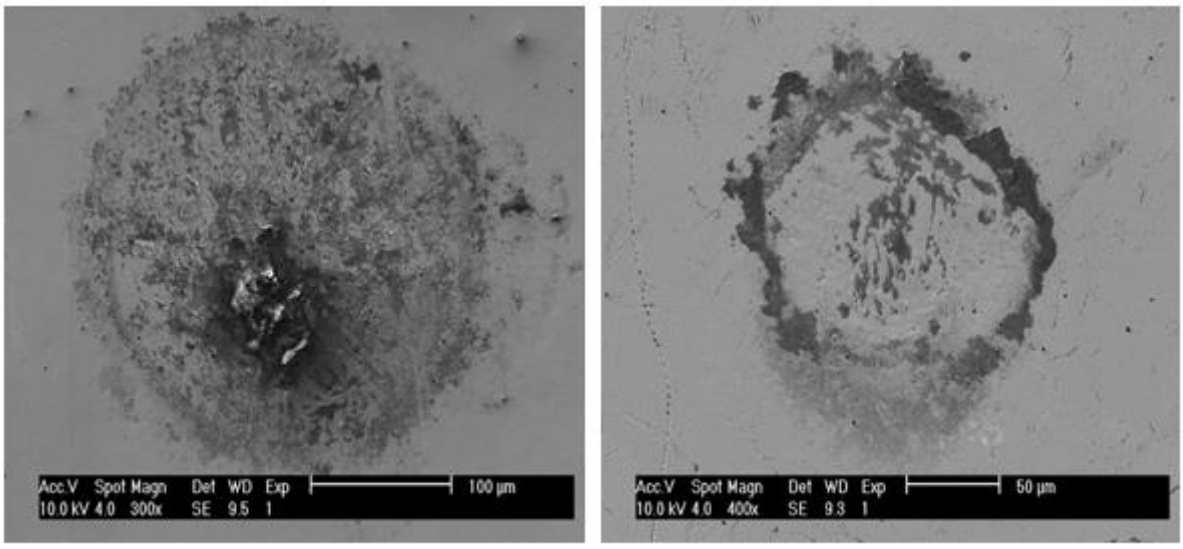

Figure 18 Cobalt-Chromium Alloy SEM images (a) with solution (b) without solution

Figure 18 explains the radial fretting profiles of CoCr by SEM images both in saline environment and in dry conditions. Stick zone is more clearly visible for the case without BSS. Surrounding the stick zone, there is slip annular region with more concentrated oxides because the density of the energy dissipated by friction is higher in effective only in this region. In the border of the slip zone, slight abrasive wear ring is clearly visible in both cases. Although the wear zone in the outer area of the contact and stick zone can be seen from the SEM images for CoCr in saline solution, micro-slip area is difficult to observe due to the presence of oxidation layer spread both in the contact zone and slip region. However it can be clearly observed mechanism more pronounced oxidation spot near in the contact centre in Figure 18 (a).

These SEM images are supportive to explain huge wear difference between saline solution and without saline solution environment for cobalt-chromium-molybdenum alloy that is shown in the Figure 17.

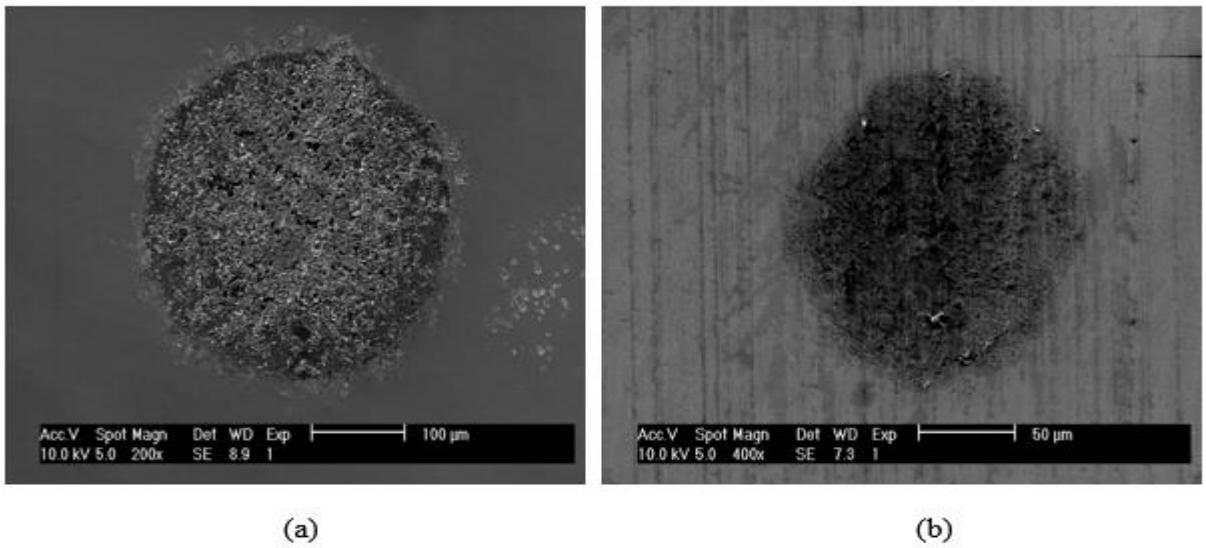

Figure 19 Titanium Grade 2 SEM images (a) with solution (b) without solution

In Figure 19(a), wear zone in the outer ring can be differentiate although wear zone is not clear for Figure 19(b) due to really small wear amount of titanium grade 2 in the air environment. The Titanium grade 2 alloy exposed saline solution Figure 19(a), has more stable oxidation layer on its surface than the other material specimens.

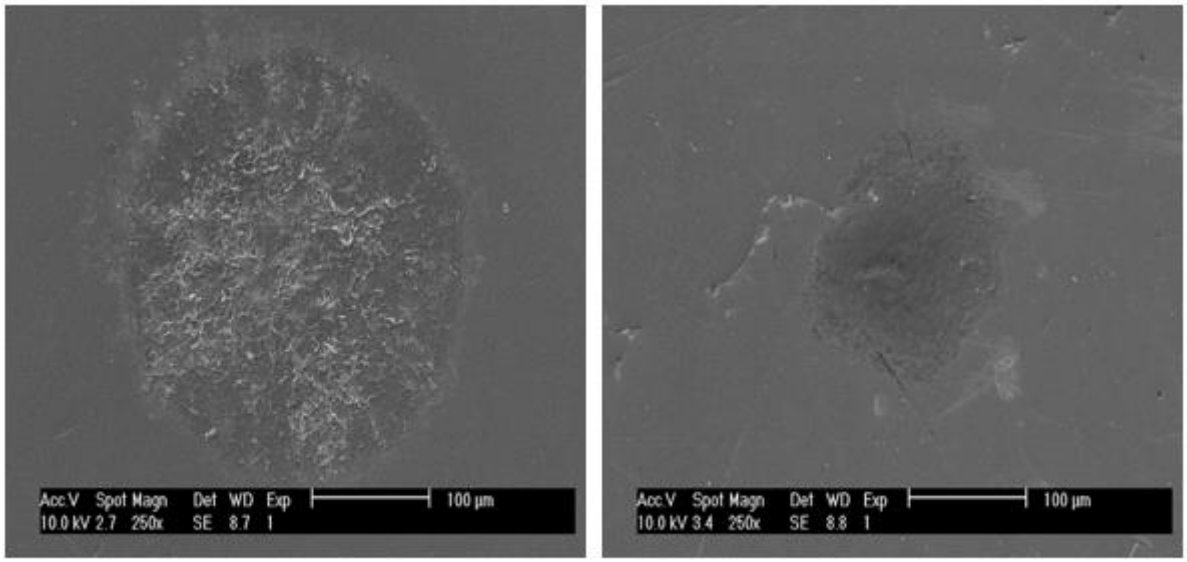

Figure 20 SEM images of Ti-6Al-4V (a) with solution (b) without solution

In Figure 20 (a), stick zone in the contact centre can be seen clearly. Although oxidation traces can be differentiated for Ti-6Al-4V in saline solution, it is much lesser than the other materials which is supportive for wear volume results showed in Figure 15.

According to the literature, Ti-6Al-4V ‘s ability to repassivate the layer of oxide decreases during fretting and this lead to extent of formation and trap of debris at the fretting zone. Additionally, presence of Al and V in Ti-6Al-4V, promote of Al_2O_3 and VO_2 in fretted zone. Due to abrasive nature of aluminium oxide, wear volume increases [62]. Also Contu et al. [63] describes that the tendency of repassivation of commercially pure titanium is higher than Ti-6Al-4V.

Air moisture can be a cause of corrosive wear during radial fretting under air only condition. This explains the higher wear volume of Ti-6Al-4V than Ti grade 2 in radial fretting under air only condition as shown in Figure 13. Even though same trend is expected between titanium alloys for radial fretting experiments, carried out in saline solution but the wear volume of Ti grade 2 is slightly higher than Ti-6Al-4V as it can be seen in Figure 15.

In overall comparison, titanium alloys have lower wear value than cobalt-chromium alloy in both environment. Titanium alloys’ wear resistance is much better than cobalt-chromium alloys in general [58]. Due to thin surface-oxide film (TiO) formation , titanium alloys are chemically resistant specifically in saline environments [23]. The difference of worn surfaces of CoCr, Ti2 and Ti-6Al-4V can be seen backscattered electron microscope images in figure 21. Therefore,

because in the case of radial fretting the contact occurs under partial slipping, the central area should remain with the oxide passivation layer and this effect can explain the better results of both titanium based tested materials.

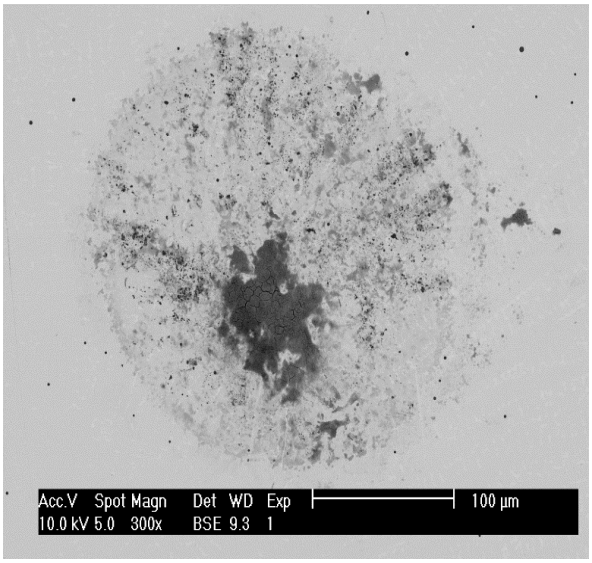

(a)

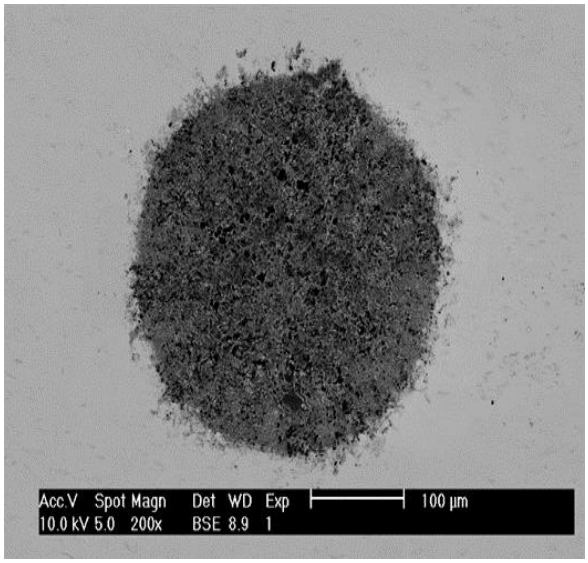

(b)

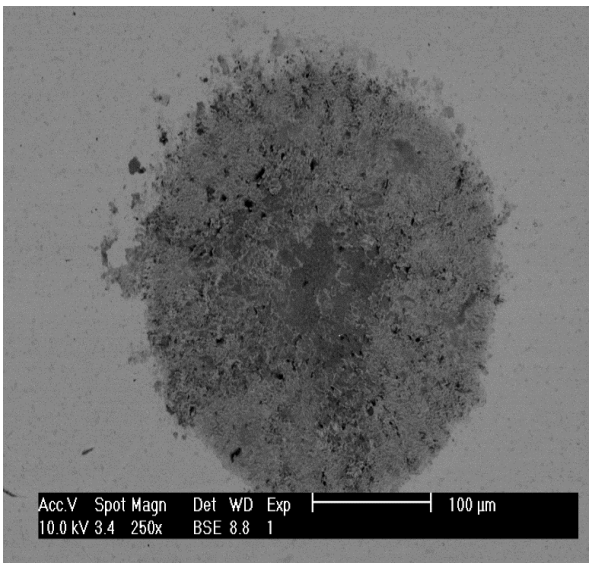

(c)

Figure 21 Backscattered electron microscope images of samples that exposed to saline solution during radial fretting experiment (a) Cobalt-chromium alloy, (b) Titanium Grade 2, (c) Ti-6Al-4V

4.6 Reciprocating Fretting Wear Results

Reciprocating wear damage is severe than radial fretting damage because the slip is extended o the entire contact area and the energy dissipated by friction is much bigger. Ploughs and detachment of particles can be observed in the wear scar of tangential fretting specimen. It is generally combination of wear mechanism like abrasive wear and oxidation. Comparison of wear volumes of three specimens under reciprocating fretting mechanism is shown in Figure 22. Ti-6Al-4V has the highest amount of wear under reciprocating fretting. Commercially pure Ti grade 2 wear volume is significantly lower than the two other specimen.

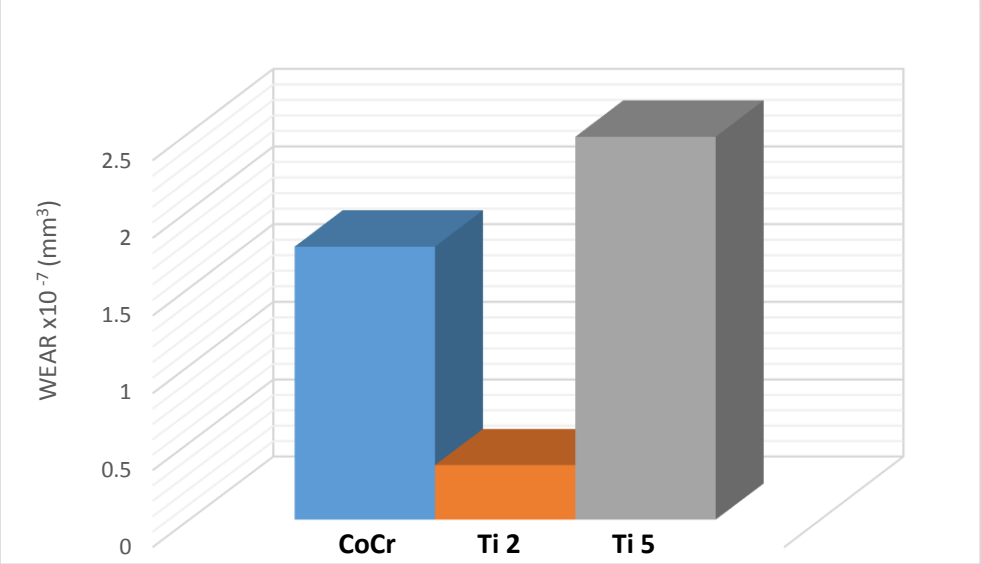

Figure 22 Reciprocating wear volume of three stem material against alumina ball under 10000 cycles

Reciprocating fretting test provide information about coefficient friction and energy dissipation which is helpful to understand materials behaviour under fretting condition.

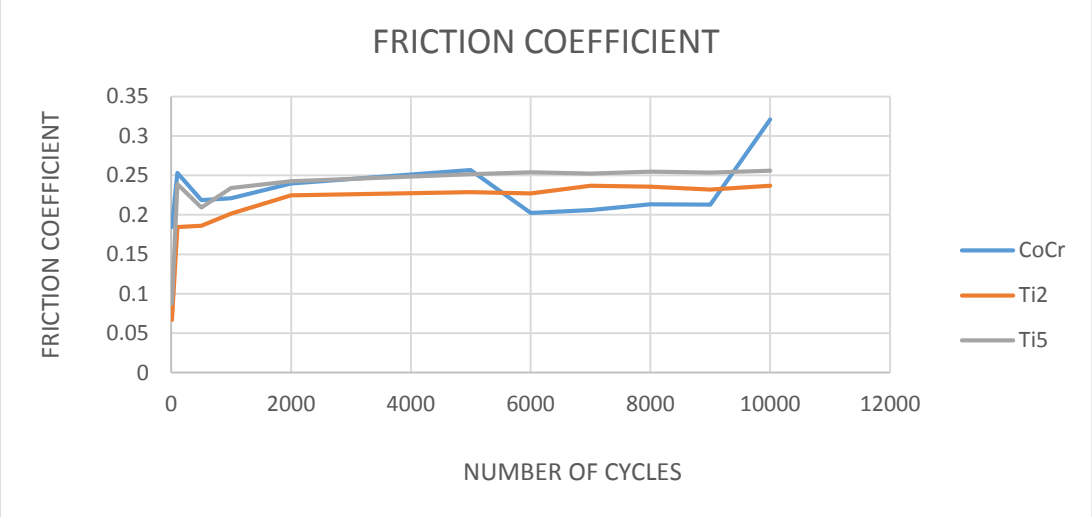

Figure 23 Comparison of coefficient friction of stem materials vs. number of cycles

From Figure 23, it is apparent that the running-in period for all the three materials is up to 500 cycles. After this period the friction value reaches steady-state for CoCr and Ti5 alloy which has a lower value than the running-in. In case of Titanium grade 2, the trend is opposite. This behaviour is probably because titanium alloy undergoes oxidation to form a TiO2 layer after around 500 cycles [64]. The TiO2 layer is known to decrease friction and cause less wear in materials [65].
Ti grade 5 has a higher friction value than Ti2 as it undergoes a larger wear as observed from Figure 22. Figure 22 shows that wear volume of the CoCr alloy is lower than Ti5 as a protective layer is formed on the surface after 5000 cycles which not only lowers the friction but also reduces the wear volume. This layer should be removed after about 9000 cycles which causes the friction to rise again and induces an increase in the wear volume.

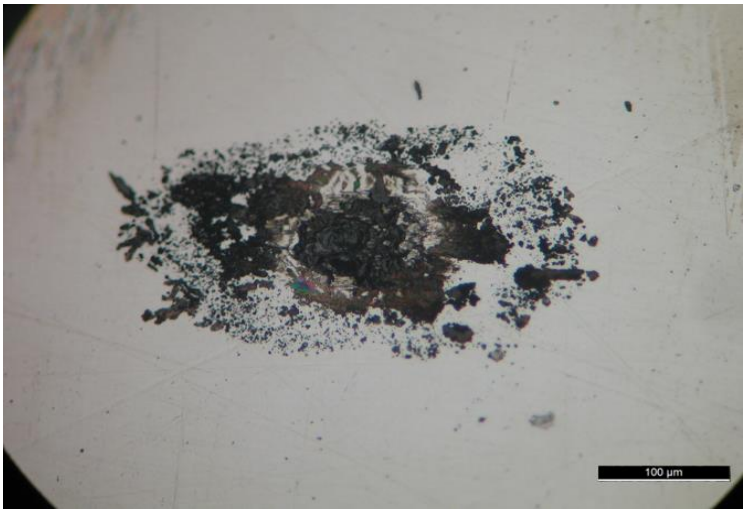

Figure 24 optical microscope image of cobalt-chromium reciprocating wear

On observing the CoCrMo surface after the experiment it was indicative of high wear and the optical microscope images of the worn surface. Figure 24 suggested the presence of an adherent oxide layer in the centre of the contact. However, the mechanism of the formation of this layer and the corresponding composition requires further SEM-EDS analysis.

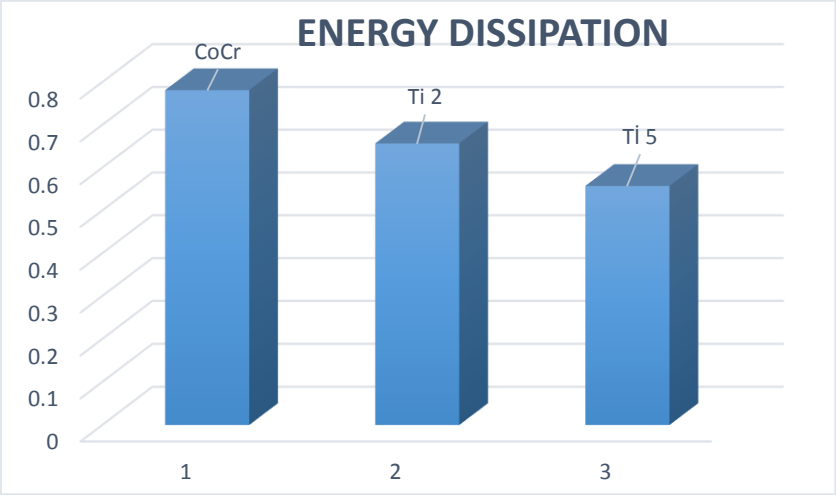

Figure 25 - Energy dissipation of the stem materials for reciprocating fretting

The energy dissipation for the CoCr alloy is the highest as correlated from the coefficient of friction curves in Figure 23. Ti grade 2 presents a slightly higher dissipation value than Ti grade 5.This was occurs because the energy dissipated is proportional to the integral of the friction force over the displacement, and because the friction is low the fretting loops should be more open in the case of the Ti grade 2 leading to an increase of the energy dissipated. However, even under higher dissipation Ti grade 2 display a lower wear volume than Ti grade 5.

CONCLUSIONS

Radial fretting test with a ball-on-flat contact was performed both in air and in balanced salt solution in order to simulate the contact between a stem and a femoral head in hip replacements. The experiment was conducted with Ti-6Al-4V, titanium grade 2 and cobalt-chromium flat specimens against an alumina ball. The wear amount induced by radial fretting on flat surfaces was calculated and the damaged surfaces were analysed to characterize fretting mechanism.

Without the balanced salt solution in the environment titanium grade 2 has the minimum wear volume loss followed by Ti-6Al-4V and cobalt-chromium respectively. In saline solution, cobalt-chromium has the highest wear as air condition but titanium grade 2 has higher amount of wear than Ti-6Al-4V. Wear is higher in balanced salt solution metallic specimens than in air. More oxidation was observed for specimens exposed to saline solution, in their SEM images.

FUTURE WORK

These results are helpful to understand the mechanism of radial fretting on some of the most common metals and alloys used as stem materials. However, the existing models are not enough to completely explain the radial fretting behaviour. Therefore, a numerical method including finite element analysis is required for interpretation for future studies. Additionally, in order to obtain a detailed understanding of the wear behaviour of materials and their contact regimes, it can be suggested that to run more radial fretting experiments with a variation of load and cycles. Furthermore, XRD and EDS characterisations can be suggested in order to analyse the oxidation and corrosion product in detail.

BIBLIOGRAPHY

[1] Dowson, D., 1992, “Friction and Wear of Medical Implants and Prosthetic Devices,” ASM Handb., **18**(Friction,Lubrication,and Wear Technology), pp. 1342–1360.

[2] “Total Hip Replacement | American Association of Hip and Knee Surgeons” [Online]. Available: http://www.aahks.org/care-for-hips-and-knees/do-i-need-a-joint-replacement/total-hip-replacement/. [Accessed: 09-Jul-2015].

[3] Holzwarth, U., and Cotogno, G., 2012, Total Hip Arthroplasty: State of the Art, Challenges and Prospects.

[4] “Total Hip Replacement-OrthoInfo - AAOS” [Online]. Available: http://www.orthoinfo.aaos.org/topic.cfm?topic=a00377. [Accessed: 11-Jul-2015].

[5] 2014, “Public and patient guide,” Natl. Jt. Regist. PATIENT Guid. TO NJR’S 11TH Annu. Rep. 2014.

[6] “Joint Revision Surgery « Orthopaedic Care Specialists” [Online]. Available: http://orthocarefl.com/?page_id=740. [Accessed: 09-Jul-2015].

[7] “Artificial hip replacement” [Online]. Available: http://www1.coe.neu.edu/~smuftu/docs/2011/ME5656_Term_Project Artificial hip replacement.pdf. [Accessed: 09-Jul-2015].

[8] Agarwal, S., 2004, “Osteolysis - basic science, incidence and diagnosis,” Curr. Orthop., **18**(3), pp. 220–231.

[9] Hallab, N., Merritt, K., and Jacobs, J., 2001, “Metal sensitivity in patients with orthopaedic implants,” J. bone Jt. Surg., **83**, pp. 428–436.

[10] “Metallosis After Hip Replacement – Symptoms, Causes & Diagnosis” [Online]. Available: http://www.drugwatch.com/hip-replacement/metallosis/. [Accessed: 09-Jul-2015].

[11] Pohler, O., 2002, “Failures of Metallic Orthopedic Implants,” ASM Handbook-vol11-Failure Analysis and Prevention, W. Becker, and R. Shipley, eds., ASM International.

[12] Gluck, T., 1890, “Autoplastik-transplantation implantation von Fremdkorpern,” Klin Wochenschr, **27**, pp. 421–427.

[13] Hughes, S., and McCarthy, I., 1998, Science Basic to Orthopaedics, WB Saunders Company Ltd:, Philadelphia.

[14] Smith-Peterson, M., 1939, “Arthroplasty of the hip, a new method,” J Bone Jt. Surg [Br], **21B**, pp. 269–288.

[15] McKee, G., and Watson-Farrar, 1966, “No Titl,” J. Bone Jt. Surg, **48B**, pp. 245–259.

[16] Charnley, J., 1967, “Total prosthetic replacement of the hip,” Physiotherapy, **53**, pp. 407–709.

[17] Ring, P., 1968, “Complete replacement arthroplasty of the hip by the Ring prosthesis,” J Bone Jt. Surg, **50B940**, pp. 720–731.

[18] Kossowsky, R., and Kossovsky, N., 1995, “Advances in Materials Science and Implant Orthopedics Surgery,” NATO ASI Ser. Kluwer Acad. Publ. Dordr., **294**, pp. 103–133.

[19] DiPisa, J. A., Sih, G. S., and Berman, A. T., 1976, “The temperature problem and the bone–acrylic cement interface of the total hip replacement,” Clin Orthop, **121**, pp. 95–98.

[20] Blanchard, C., Medlin, D. ., and Shetty, R., 2003, “Joint Replacements and Bone Resorption: Pathology and Clinical Practice,” Adv. Met.

[21] Mears, D. ., 1979, Materials and Orthopaedic Surgery, Williams and Wilkens Co.

[22] Black, J., 1988, Orthopaedic Biomaterials in Research and Practice, Churchhill Livingstone.

[23] Donachie, M., 2000, Titanium: A Technical Guide, ASM International.

[24] Ratner, B. ., Hoffman, A. ., Schoen, F., and Lemons, J., 1996, Biomaterials Science: An Introduction to Materials in Medicine, Academic Press.

[25] Shaffer, S., and Glaeser, W., 1996, “Fretting Fatigue,” ASM Handbook-Vol 19, ASM International.

[26] Zhu, M. H., and Zhou, Z. R., 2011, “On the mechanisms of various fretting wear modes,” Tribol. Int., **44**(11), pp. 1378–1388.

[27] Mindlin, R., and Deresiewicz, H., 1953, “Elastic spheres in contact under varying oblique forces,” J. Appl. Mech., **20**, pp. 327–344.

[28] [Johnson, K., 1961, “Energy dissipation at spherical surfaces in contact transmitting oscillating forces,” J. Mech. Eng. Sci., **3**, p. 362.

[29] Zhu, M. H., Zhou, Z. R., Kapsa, P., and Vincent, L., 2001, “An experimental investigation on composite fretting mode,” Tribol. Int., **34**(11), pp. 733–738.

[30] Mindlin, R., 1949, “Compliance of elastic bodies in contact,” J. Appl. Mech., **16**, pp. 259–268.

[31] Vingsbo, O., and Söderberg, S., 1988, “On fretting map,” Wear, (126), pp. 131–147.

[32] Zhou, Z. R., Nakazawa, K., Zhu, M. H., Maruyama, N., Kapsa, P., and Vincent, L., 2006, “Progress in fretting maps,” Tribol. Int., **39**(10), pp. 1068–1073.

[33] Zheng, J., Luo, J., Mo, J., Peng, J., XS, J., and Zhu, M. H., 2010, “Fretting wear behaviours of a railway axle steel,” Tribol. Int., (43), pp. 906–911.

[34] Zhu, M. H., and Zhou, Z. R., 2001, “An experimental study on radial fretting behaviour,” Tribol. Int., **34**(5), pp. 321–326.

[35] Zhu, M. H., Yu, H. Y., and Zhou, Z. R., 2005, “Radial fretting behaviours of dental feldspathic ceramics against different counterbodies,” Wear, pp. 996–1004.

[36] Zhu, M. H., Yu, H. Y., and Zhou, Z. R., 2006, “Radial fretting behaviours of dental ceramics,” Tribol. Int., **39**(10), pp. 1255–1261.

[37] Mohrbacher, H., Celis, J., and Roos, J., 1995, “Laboratory testing of displacement and load induced fretting,” Tribol. Int., **28**(5), pp. 269–278.

[38] Ciornei, F., Irimescu, L., and Diaconescu, E. N., 2006, “Upon Radial Fretting of Dissimilar Materials,” Ann. Univ. “Dunărea Jos “ Galaţi, **2006**(Xii), pp. 134–139.

[39] Pereira, J. P. R., “Fretting Por Expansao Radial: Um abordagem experimental.”, Master Thesis of Mechanical Engineering in University of Coimbra

[40] Reza, H., Hosseinzadeh, S., Eajazi, A., and Shahi, A. S., 2012, “The Bearing Surfaces in Total Hip Arthroplasty – Options, Material Characteristics and Selection,” Recent Adv. Arthroplast., pp. 163–210.

[41] Buford, A., and Goswami, T., 2004, “Review of wear mechanisms in hip implants,” Mat Des, **25**, pp. 385–393.

[42] Howcroft, D., 2008, “Bearing surfaces in the young patient: out with the old and in with the new?,” Curr. Orthop., **22**, pp. 177–184.

[43] Long, M., and Rack, H. ., 1998, “Titanium alloys in total joint replacement—a materials science perspective,” Biomaterials, **19**(18), pp. 1621–1639.

[44] Fraker, A., 1987, “Corrosion of Metallic Implants and Prosthetic Devices,” ASM Handbook-Vol 13-Corrosion, ASM International.

[45] Davis, J. R., ed., 2003, Handbook of Materials for Medical Devices, Ohio,USA.

[46] Donachie, M., 1998, Metals Handbook Desk Edition, ASM International.

[47] D, W., 1990, “Biocompatibility: An Overview,” Concise Encycl. Med. Dent. Mater., pp. 51–59.

[48] “DoITPoMS - TLP Library Structure of bone and implant materials - Materials selection of femoral stem component” [Online]. Available: http://www.doitpoms.ac.uk/tlplib/bones/stem.php. [Accessed: 14-Jun-2015].

[49] “CP Titanium Grade 2” [Online]. Available: http://cartech.ides.com/datasheet.aspx?i=101&E=266. [Accessed: 15-Jun-2015].

[50] “ASM Material Data Sheet” [Online]. Available: http://asm.matweb.com/search/SpecificMaterial.asp?bassnum=MTP641. [Accessed: 14-Jun-2015].

[51] Ohmori, H., Katahira, K., Nagata, J., Mizutani, M., K., and J., 2002, “Improvement of corrosion resistance in metallic biomaterials using a new electrical grinding technique,” Ann. CIRP 51/1, pp. 491–494.

[52] SMITH, G. K., “ORTHOPAEDIC BIOMATERIALS” [Online]. Available: http://cal.vet.upenn.edu/projects/saortho/chapter_13/13mast.htm. [Accessed: 14-Jun-2015].

[53] Rothman, M., Zordan, Z., and Muzyka, D., 1984, Role of Refractory Elements in Cobalt-Base Alloys, in Refractory Alloying Elements in Superalloys, American Society for Metals.

[54] Davis, J., Destefani, J., and Frissell, H., 1987, “ASM METALS HANDBOOK VOLUME 13 Corrosion,” ASM International, 1987,.

[55] “DoITPoMS - TLP Library Structure of bone and implant materials - Materials selection of femoral head and acetabular cup components” [Online]. Available: http://www.doitpoms.ac.uk/tlplib/bones/head.php. [Accessed: 15-Jun-2015].

[56] Gadelmawla, E., Koura, M., Maksoud, T., Flewa, I., and Soliman, H., 2002, “Roughness parameters,” J. Mater. Process. Technol., **123**(1), pp. 133–145.

[57] Voort, G., ed., 2004, “Contrast Enhancement and Etching,” ASM Handbook-Vol 09-Metallography and microstructure, ASM International, pp. 294–312.

[58] Medlin, D. ., and Compton, R., 2004, “Metallography of Biomedical Orthopedic Alloys,” pp. 961–968.

[59] Gammon, L., Briggs, R., Packard, J., Batson, K., Boyer, R., and Domby, C., 2004, “Metallography and Microstructures of Titanium and Its Alloys,” ASM Handbook-Vol 09-Metallography and microstructure, ASM International, pp. 899–917.

[60] Esteves, M. A. P., “Study of Fretting behaviour on automotive electrical contacts.”, Projecto de Tese Final,Department of Mechanical Engineering,Universidade

[61] Sykaras, N., Lacopin, A. M., and Maker, V. ., 2000, “Implant materials, designs, and surface topographies: their effect on osseointegration,” Int. J. Oral Maxillofac Implant., **15**, pp. 675–690.

[62] Sivakumar, B., Kumar, S., and Narayanan, T. S. N. S., 2011, “Comparison of fretting corrosion behaviour of Ti-6Al-4V alloy and CP-Ti in Ringer’s solution,” Tribol. - Mater. Surfaces Interfaces, **5**(4), pp. 158–164.

[63] Contu, F., Elsener, B., and Bohni, H., 2004, “A study of the potentials achieved during mechanical abrasion and the repassivation rate of titanium and Ti6Al4V in inorganic buffer solutions and bovine serum,” Electrochim. Acta, **50**(1), pp. 33–41.

[64] Choubey, A., Basu, B., and Balasubramaniam, R., 2005, “Tribological behaviour of Ti-based alloys in simulated body fluid solution at fretting contacts,” Trends Biomater.

Artif. Organs, **18**(2), pp. 141–147.

[65] Rahmani, E., Ahmadpour, A., and Zebarjad, M., 2011, “Influence of SiO 2 in TiO 2 matrix on tribological properties of TiO 2,” 7th Int. Chem. Eng. Congr. Exhib.

APPENDIX

PRELIMINARY RADIAL FRETTING EXPERIMENT TEST RESULTS

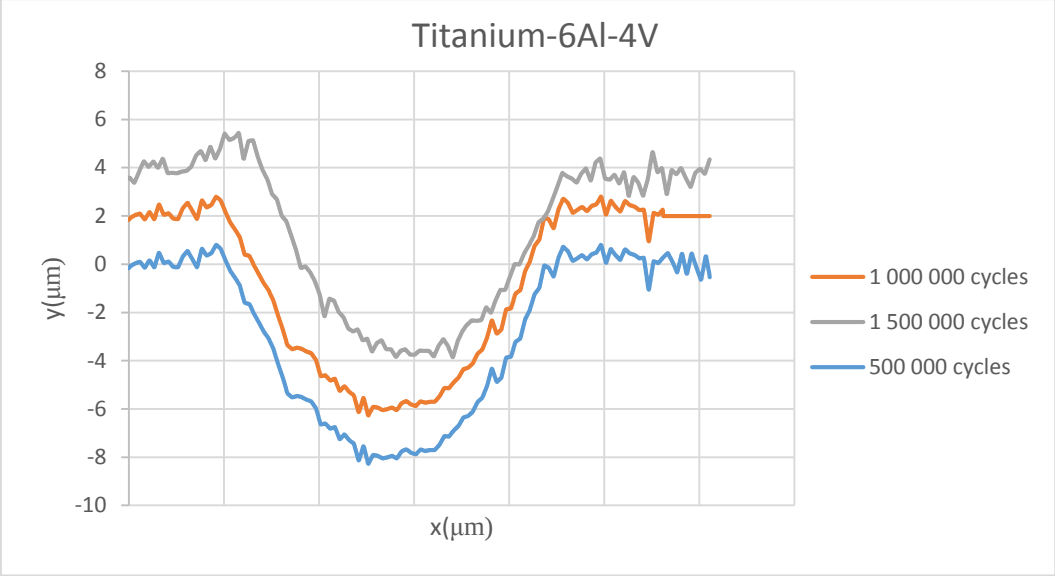

Figure 26– 2D profiles of Ti-6Al-4V alloys under radial fretting with different cycles

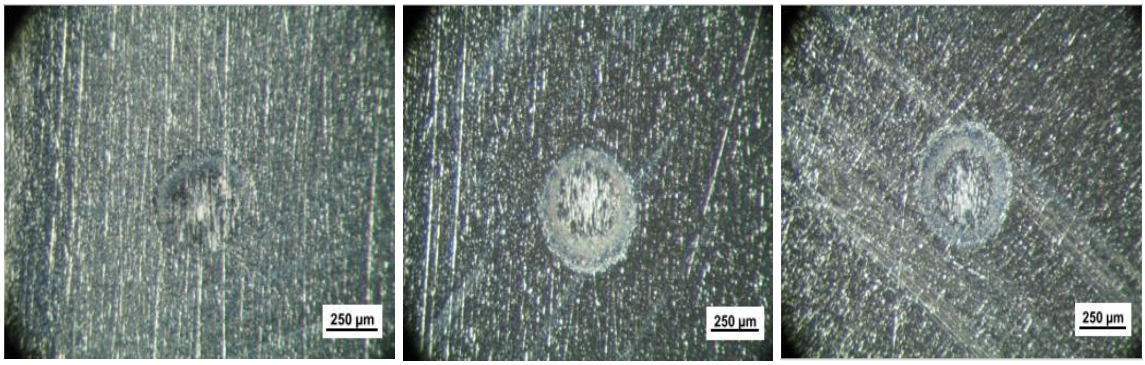

(a) (b) (c)

Figure 27- Optical microscope images of Ti-6Al-4V (a) $5x10^5$ cycles, (b) $1x10^6$ cycles, (c) $1,5x10^6$ cycles